

Letter

Multiple Filamentation Effects on THz Radiation Pattern from Laser Plasma in Air

Aleksandr Ushakov ^{1,*} , Pavel Chizhov ¹ , Vladimir Bukin ¹, Daniil Shipilo ^{2,3} , Nikolay Panov ^{2,3}, Olga Kosareva ^{2,3}  and Sergey Garnov ¹

¹ Prokhorov General Physics Institute of the Russian Academy of Sciences, 119991 Moscow, Russia; pvch@kapella.gpi.ru (P.C.); vbkn@kapella.gpi.ru (V.B.); garnov@kapella.gpi.ru (S.G.)

² Faculty of Physics and International Laser Center, Lomonosov Moscow State University, 119991 Moscow, Russia; schipilo.daniil@physics.msu.ru (D.S.); napanov@physics.msu.ru (N.P.); kosareva@physics.msu.ru (O.K.)

³ P. N. Lebedev Physical Institute of the Russian Academy of Sciences, 119991 Moscow, Russia

* Correspondence: ushakov.aleksandr@physics.msu.ru; Tel.: +7-499-503-87-77/4-13

Abstract: An experimental study of few filaments interaction impact on the terahertz radiation pattern has demonstrated that interaction of two close propagating beams leads to formation of a superfilament-like structure with on-axis terahertz yield. Mutual delay between two beamlets tilts the output intensity front of THz emission.

Keywords: terahertz radiation; laser plasma; filamentation



Citation: Ushakov, A.; Chizhov, P.; Bukin, V.; Shipilo, D.; Panov, N.; Kosareva, O.; Garnov, S. Multiple Filamentation Effects on THz Radiation Pattern from Laser Plasma in Air. *Photonics* **2021**, *8*, 4. <https://doi.org/10.3390/photonics8010004>

Received: 6 December 2020

Accepted: 23 December 2020

Published: 25 December 2020

Publisher's Note: MDPI stays neutral with regard to jurisdictional claims in published maps and institutional affiliations.



Copyright: © 2020 by the authors. Licensee MDPI, Basel, Switzerland. This article is an open access article distributed under the terms and conditions of the Creative Commons Attribution (CC BY) license (<https://creativecommons.org/licenses/by/4.0/>).

1. Introduction

Development of terahertz (THz) radiation sources and detectors is one of the key scientific directions nowadays, due to the possibility of applying THz techniques in different areas of science and technology [1]. Laser plasma is a promising source of THz radiation due to ultrabroad spectrum 0.1–200 THz [2], relatively high peak fields [3], and the possibility of forming a source in front of a studied object avoiding losses due to propagation in air [4–6]. These sources have been studied over the last three decades and the questions of generation mechanisms [5,7,8], efficiency [8–11], polarization dependencies [12–17], and output diagram [18–28] have been considered. The application of focused THz emission from sources is fruitful for optical pump-THz probe spectroscopy [29,30] and also for the study of nonlinear THz properties of matter, for example, by z-scan technique [31], thus, it is necessary to know the THz radiation spatial distribution for the estimation of electric THz field. However, strong angular divergence and conical structure of the THz emission [18–28] from the single filament have been observed and they reduce its applicability. For the single filament, it is possible to control the spatial distribution of THz emission by application of tight focusing of the pump beam [32]. In addition, it is possible to form several plasma channels, and thus transform an output THz emission pattern. At higher laser pulse energies, the formation of several sources may appear due to multiple filamentation or superfilamentation [33–38]. Superfilamentation is a specific regime of interaction of several filaments, when the last one forms a single high intense channel. High intensity in the superfilament leads to increasing of nonlinear processes and transformation of angular and frequency-angular output emission [31–33]. In the case of multiple filamentation, THz emission is a result of interaction of several plasma sources. The theory of this question has been studied in literature [39,40], however there is no experimental evidence. Thus, it is important to study the impact of several filaments on the output THz emission spatial distribution. It is possible to create several filaments simultaneously by regularization of optical pump beam using amplitude or phase masks [36,37]. Interference of THz radiation from these filaments or superfilaments may lead to enhancement of THz emission in on-axis direction. Therefore, it is important to clarify the optimized condition

of THz beam generation and to develop ways to control the spatial distribution of THz emission by the two-color scheme. In this paper, we experimentally study THz emission pattern from complex laser plasma sources formed by several plasma channels.

2. Experimental Setup

In this paper, we used an amplitude mask for modulation of laser beam. To study the impact of separate plasma channels on the output spatial distribution of THz emission, the following experimental setup was constructed (see Figure 1). The radiation of a Ti: Sapphire laser (central wavelength 800 nm, pulse energy up to 2.9 mJ, duration 50 fs, diameter 12 mm at e^{-2} level, repetition rate 1 kHz) was divided into three beams as follows:

- (1) The pump beam, which generated plasma, the THz source;
- (2) The first probe beam for EO system THz radiation registration;
- (3) The second probe beam for diagnostic of plasma channel.

The energy of the pump pulse was varied by means of a half-wave plate and a polarizer that transmitted horizontally polarized radiation. The laser radiation in the pump beam was partially converted into second harmonic by a BBO crystal (I type, $10 \times 10 \times 0.1 \text{ mm}^3$). To increase the efficiency of THz generation, polarizations of the fundamental and the second harmonic radiation were aligned by a phase plate ($\lambda_1/2 + \lambda_2$, where λ_1 is the fundamental wavelength and λ_2 is the second harmonic) and the group delay between them was compensated by a compensator plate (calcite plate). An off-axis parabolic mirror with a focal length of 200 mm focused the two-color beam into the atmospheric air. A fluorescent plasma channel was 10 mm in length for the free pump beam (without a mask) focused.

To form a regularized bundle of filaments, a mask was placed before the parabolic mirror. The mask was a metal plate with two holes 5 mm in diameter at a distance of 6 mm between their centers. The mask center was set on the laser beam center to provide approximately equal energy in two beamlets. We studied both vertical and horizontal orientation of the mask holes (orthogonal to and coincident with the plane of angular measurements, respectively).

To produce two independent filaments, we covered half of the pump beam by a quartz plate placed in front of a BBO crystal. As a result, one half of the laser beam was delayed by ~ 250 fs from the other half. The interaction of two beamlets, thus, did not take place as the duration of laser pulses was significantly lesser than delay between them.

A standard electro-optical (EO) detector consisting of a ZnTe crystal (cut $\langle 110 \rangle$, $3 \times 3 \times 1 \text{ mm}^3$), a quarter-wave plate, a polarization divider (Glan–Taylor prism), and two photodiodes was used to measure THz pulse waveform. The detection crystal was placed at a distance of 200 mm from the center of the plasma channel at different angles α to the optical axis of the pump beam in the horizontal plane. To detect THz radiation, the first probe beam was directed to the ZnTe crystal. The THz waveforms were recorded by scanning over the delay of the first probe beam (by using delay Line 1). Calibration of the EO detector signal was carried out for each angle by measuring the maximum signal amplitude on one of the photodiodes (with the second one closed). The Fourier transformation of THz waveforms provided the spectrum of THz radiation at the corresponding angle α ; all together they were assembled to the frequency-angular distribution [33]. For the measurements of angular distribution of THz power without spectral resolution, we used a Golay cell (Tydex GC-1P) instead of an EO detector. We used a gated laser operation to provide 20 Hz low-frequency modulation for the THz power measurements.

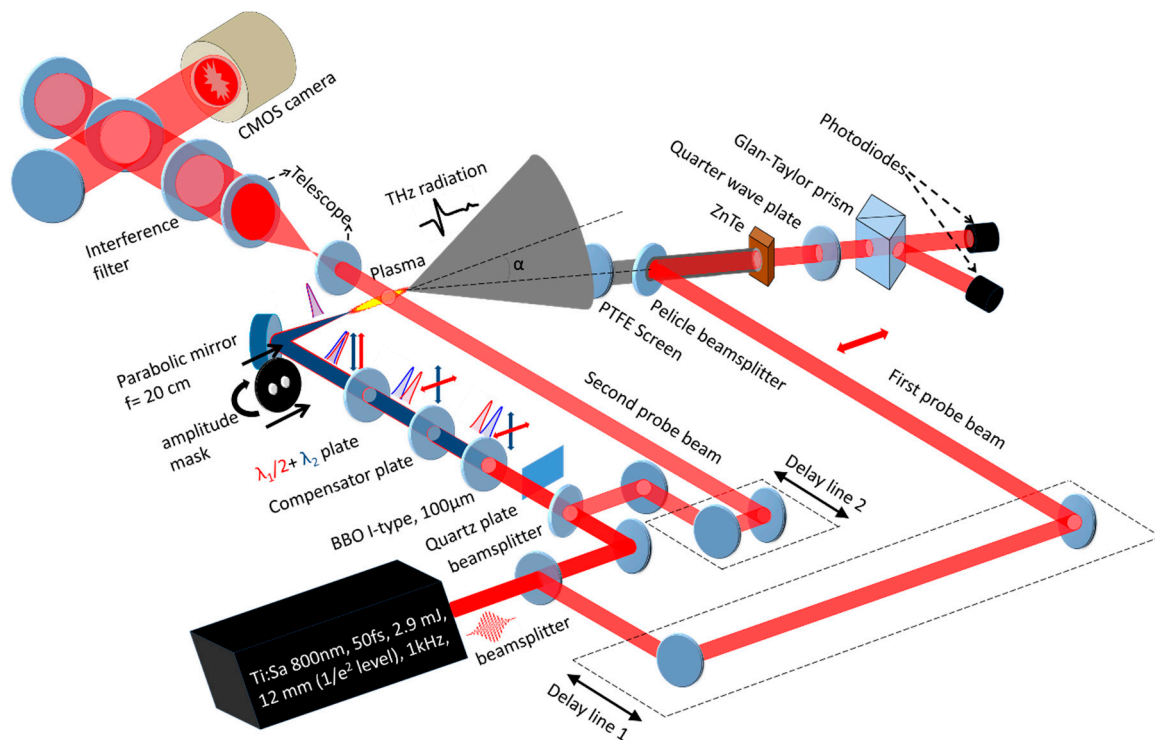


Figure 1. Experimental setup.

The pump-probe interferometry was used to characterize the plasma channel. The second probe beam passed through the optical delay Line 2, and then through the central part of the plasma channel perpendicularly to the pump beam axis. The probe beam refracted on the plasma was telescoped to a Michelson interferometer with a slightly tilted beam in one of the arms. Tilt is enabled to control the interference stripes period and to form two shifted images of plasma channel (with each beam as a reference for another one). Two shifted images (beams) of the studied region of the plasma channel were formed on a CMOS camera matrix (from each arm of the interferometer). An interference filter (802 nm central transmittance wavelength with bandpass 5 nm FWHM) was inserted into the beam to increase the contrast area of the interference bands. A phase shift in the plasma was probed right after ionization. Under the horizontal orientation of amplitude mask holes alignment by probe beam leads to accumulating of phase shift of several filaments in the interferogram. Thus, the extraction of electron concentration in plasma channel becomes impossible. Therefore, we provide interferometry diagnostics only for vertical orientation of amplitude mask holes.

3. Results and Discussions

The experiments were carried out with radiation energy of the pumping laser beam 0.95 mJ in front of the parabolic mirror (after the mask when it was used), i.e., at a peak pulse power of about 20 GW. This value is two times larger than the critical power for self-focusing [38]. The following three versions of the plasma source were implemented:

1. Single plasma channel formed by free beam without a mask (see Figure 2a).
2. Interaction of filaments formed after two mask holes (for vertical and horizontal orientation of the holes). This corresponds to the registration of three channels in the phase shift distribution. The brightest central plasma channel corresponds to the superfilament-like structure, Figure 2b.
3. Independent formation of two filaments due to a delay of ~ 250 fs between two beamlets (also for vertical and horizontal orientation of the mask holes), Figure 2c.

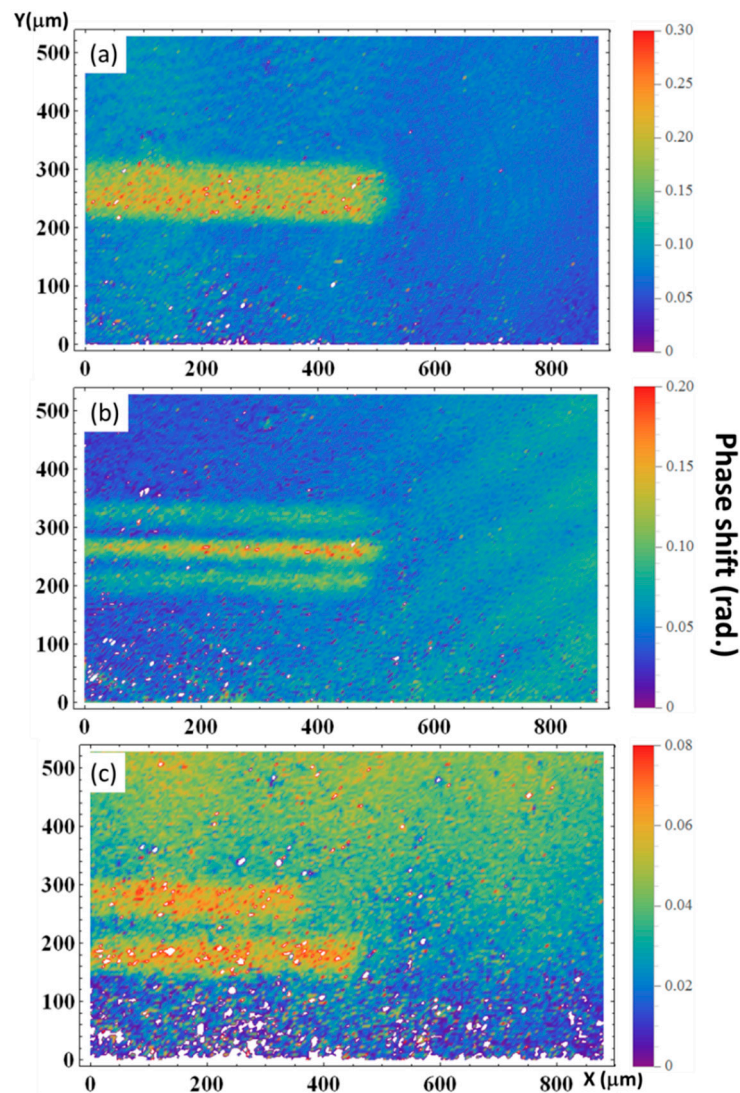


Figure 2. Phase shift in plasma channel registered by means of interferometry. (a) Beam without a mask; (b) A vertical orientation of the amplitude mask, simultaneous pulses, and interaction of filaments; (c) A vertical orientation of the amplitude mask, delayed pulses, thus, independent filaments. The pump pulse energy in all cases is 0.95 mJ. For all distributions, the probe delay was set at “0” position for the central region of image.

For the estimation of electron concentration of plasma, we assume an axial symmetry for each channel. Thereafter, we apply the reverse Abel transformation for each plasma channel to extract the distribution of refractive index in filaments and, consequently, the plasma density distribution. The peak plasma density was $1.4 \times 10^{18} \text{ cm}^{-3}$ in Figure 2a, $2.3 \times 10^{18} \text{ cm}^{-3}$ in Figure 2b ($5 \times 10^{17} \text{ cm}^{-3}$ for secondary peaks), and $7 \times 10^{17} \text{ cm}^{-3}$ in Figure 2c panel.

Figure 3 compares angular distributions of THz power measured by the Golay cell for the described cases, for a single beamlet (one hole closed on the inserted mask) and its counterpart when the mask is rotated by 90° to align holes in the horizontal plane. The free beam provides the highest THz power. Three filaments formed under interaction of two beamlets provide a lower THz yield. Two independent delayed filaments provide almost the same minimal output as a single beamlet. Horizontal and vertical orientations of the mask holes do not make a notable distinction for any case, thus, one can suppose that the structure of plasma channels does not change significantly. The resulting diagram from two delayed filaments is not an arithmetical sum of THz yields from each channel. This

shows the significant interference between these two sources. The directional diagram has a maximum at +5 degrees, with no symmetric THz yield for −5 degrees. It corresponds to the tilted front of intensity due to delayed THz emission from the one of the plasma sources.

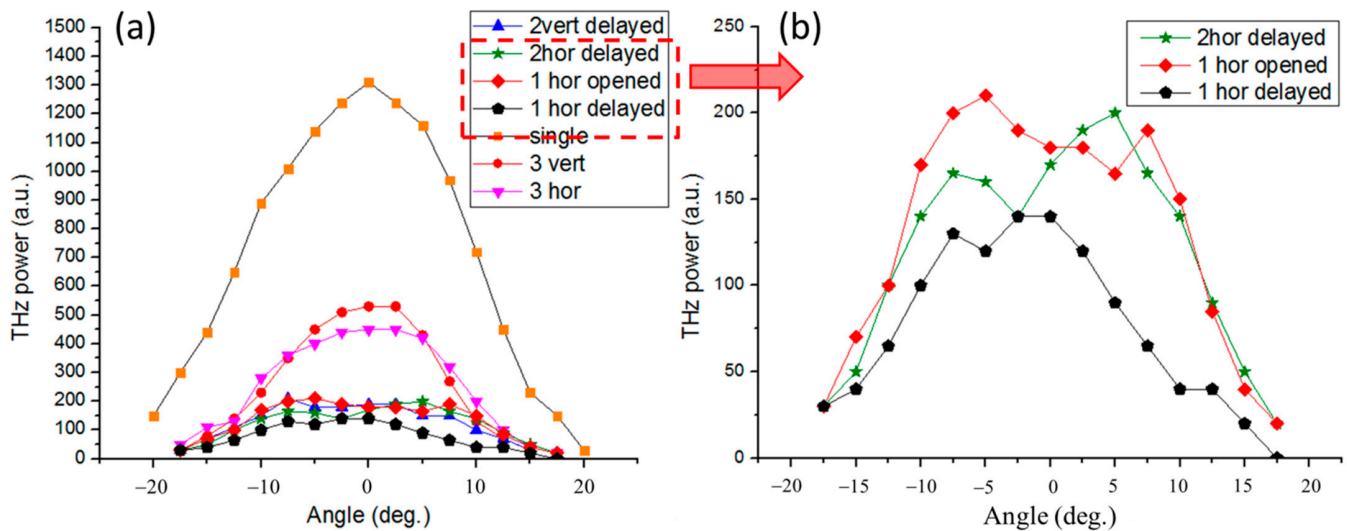


Figure 3. Angular distributions of THz power for different filament configurations. (a) Two vertically oriented filaments with mutual delay (blue triangle), 2 horizontally oriented filaments with mutual delay (green star), 1 filament without quartz plate (red rhombus), 1 filament with quartz plate (black pentagon), 1 filament without a mask (full laser beam) (orange circle), 3 vertically oriented filaments (red circle), 3 horizontally oriented filaments (purple circle); (b) Angular distribution for three selected cases.

Figure 4 shows the frequency-angular spectra of THz radiation retrieved from EO detection in the horizontal plane, for filamentation modes shown in Figure 2. In the case when the mask was not used (Figure 4a), the frequency-angular distribution is typical for the moderate focusing mode of the two-color femtosecond pulse [20,21,24,26,33]. THz radiation has a flat distribution of amplitude with emerging of conical structure with an opening angle of 5–10°. Measured frequency-angular spectra of THz radiation of two-color filament are in reasonable agreement with the results of experiments and simulations performed earlier [33].

The frequency-angular spectrum of THz radiation from superfilament-like structure is shown in Figure 4, for horizontal (Figure 4b) and vertical (Figure 4c) orientation of the mask. In contrast to the previous case, the superfilament-like plasma channels form a new THz component propagating on the beam axis (at an angle of 0°). Nevertheless, surrounding rings with a divergence angle of 5–10° also appear.

Numerical simulations [39] have proposed that the interference of THz fields from several sources with cone emission pattern each resulted in a conical spatial distribution surrounded by sidelobes, but not an axial component. In experiments [40] with two parallel non-interactive structures, only the conical THz field spatial distribution was observed. However, we experimentally verified and confirmed the relationship between the appearance of the axial component in the frequency-angular distribution of THz radiation and the interaction of filaments. In fact, the interaction of filaments from different holes in the mask can be significantly limited by delaying femtosecond radiation, passing through one hole, at ~250 fs relative to the radiation passing through the other hole. In this case, the filaments formed in a pulse with the duration of 50 fs do not interact anymore, however, THz pulses with duration of 1–2 ps (this THz pulse duration was obtained in experiments) can overlap in time and space and interfere with each other. Figure 4d,e shows the frequency-angular spectra of THz radiation in the case of two delayed filaments for horizontal and vertical orientation of the mask, respectively. In both cases, the conical

spatial distribution prevails, and the axial component is minor as compared with the case of superfilament-like structure, Figure 4b,c.

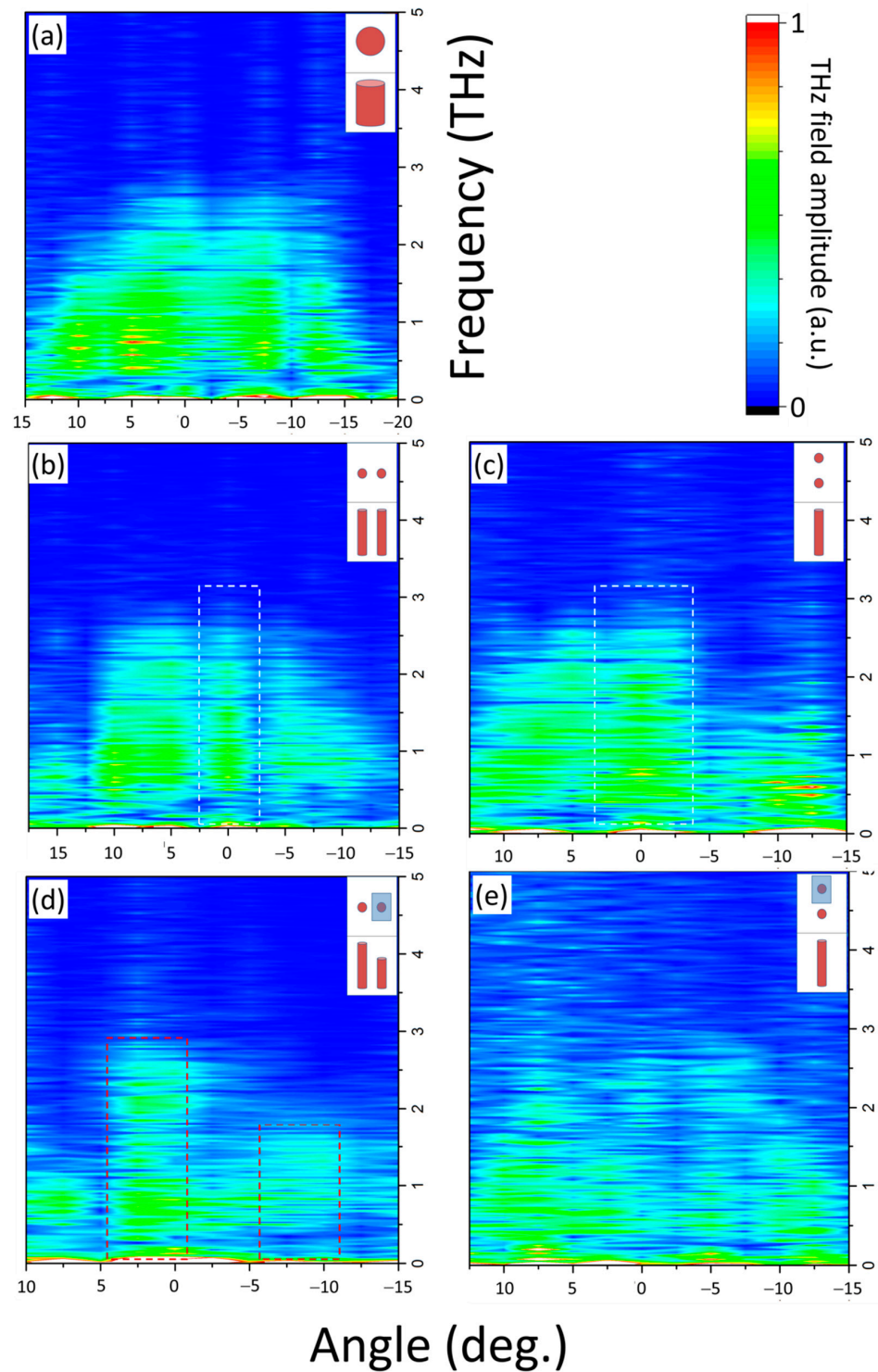


Figure 4. Frequency-angular distributions of THz emission. (a) free beam without a mask; (b,c) Two beamlets regularized forming superfilament-like structure; (d,e) Two independent delayed filaments. Measurements (b,d) were made with horizontal orientation of mask holes and (c,e) with vertical one. White rectangles in (b,c) highlight the component of THz radiation that propagates along the axis of the laser beam, red rectangles in (d) highlight the feature of THz emission from two delayed beamlets.

4. Conclusions

Thus, the possibility controlling THz emission spatial distribution for composite laser-plasma source has been demonstrated using amplitude mask for laser beam and introducing delay between beamlets. The interaction of two non-delayed beamlets leads to formation of a complex superfilament-like structure, which is characterized by a bright component of THz emission propagating along the axis. The introduction of delay between two beamlets shifts the maximum in angular and frequency-angular distributions. However, it should be noted that the spatial modulation decreases the total energy of THz emission, as the highest THz yield is observed for the single filament. The ring component, corresponding to THz radiation of the original filaments, is also present. These results can be useful for high power broadband laser-plasma THz sources and for control of the THz pattern.

Author Contributions: A.U., P.C., and V.B. performed experiment and data processing; D.S., N.P., and O.K. performed data analysis; V.B., O.K., and S.G. supervised the whole study. All authors have read and agreed to the published version of the manuscript.

Funding: This work was supported by the Ministry of Science and Higher Education of the Russian Federation (project 075-15-2020-790).

Conflicts of Interest: The authors declare no conflict of interest.

References

1. Zhang, X.-C.; Xu, J. *Introduction to THz Wave Photonics*; Springer: New York, NY, USA, 2010; pp. 10–200.
2. Matsubara, E.; Nagai, M.; Ashida, M. Ultrabroadband coherent electric field from far infrared to 200 THz using air plasma induced by 10 fs pulses. *Appl. Phys. Lett.* **2012**, *101*, 011105. [[CrossRef](#)]
3. Zhang, X.C.; Shkurinov, A.; Zhang, Y. Extreme terahertz science. *Nat. Photonics* **2017**, *11*, 16–18. [[CrossRef](#)]
4. Hamster, H.; Sullivan, A.; Gordon, S.; White, W.; Falcone, R.W. Subpicosecond, Electromagnetic Pulses from Intense Laser-Plasma Interaction. *Phys. Rev. Lett.* **1993**, *71*, 2725–2728. [[CrossRef](#)] [[PubMed](#)]
5. Cook, D.J.; Hochstrasser, R.M. Intense terahertz pulses by four-wave rectification in air. *Opt. Lett.* **2000**, *25*, 1210–1212. [[CrossRef](#)]
6. Chizhov, P.A.; Ushakov, A.; Bukin, V.V.; Garnov, S.V. Terahertz radiation from extended two-colour air filaments. *Laser Phys. Lett.* **2019**, *16*, 075301. [[CrossRef](#)]
7. Chizhov, P.A.; Volkov, R.V.; Bukin, V.V.; Ushakov, A.A.; Garnov, S.V.; Savel'ev-Trofimov, A.B. Generation of terahertz radiation by focusing femtosecond bichromatic laser pulses in a gas or plasma. *Quantum Electron.* **2013**, *43*, 347–349. [[CrossRef](#)]
8. Kim, K.Y.; Glowina, J.H.; Taylor, A.J.; Rodriguez, G. Terahertz emission from ultrafast ionizing air in symmetry-broken laser fields. *Opt. Express* **2007**, *15*, 4577–4584. [[CrossRef](#)]
9. Löffler, T.; Roskos, H.G. Gas-pressure dependence of terahertz-pulse generation in a laser-generated nitrogen plasma. *J. Appl. Phys.* **2002**, *91*, 2611–2614. [[CrossRef](#)]
10. Volkov, R.V.; Chizhov, P.; Ushakov, A.; Bukin, V.V.; Garnov, S.V.; Savel'ev, A. Optimal polarization of a two-colored pump for terahertz generation with a phase-unstable scheme. *Laser Phys.* **2015**, *25*, 065403. [[CrossRef](#)]
11. Ponomareva, E.A.; Tsytkin, A.N.; Smirnov, S.V.; Putilin, S.E.; Yiwen, E.; Kozlov, S.A.; Zhang, X.-C. Double-pump technique—One step closer towards efficient liquid-based THz sources. *Opt. Express* **2019**, *27*, 32855–32862. [[CrossRef](#)]
12. Xie, X.; Dai, J.; Zhang, X.-C. Coherent Control of THz Wave Generation in Ambient Air. *Phys. Rev. Lett.* **2006**, *96*, 075005. [[CrossRef](#)] [[PubMed](#)]
13. Houard, A.; Liu, Y.; Prade, B.; Mysyrowicz, A. Polarization analysis of terahertz radiation generated by four-wave mixing in air. *Opt. Lett.* **2008**, *33*, 1195–1197. [[CrossRef](#)] [[PubMed](#)]
14. Manceau, J.-M.; Massaouti, M.; Tzortzakis, S. Coherent control of THz pulses polarization from femtosecond laser filaments in gases. *Opt. Express* **2010**, *18*, 18894–18899. [[CrossRef](#)] [[PubMed](#)]
15. Kosareva, O.G.; Panov, N.A.; Volkov, R.V.; Andreeva, V.; Borodin, A.V.; Esaulkov, M.N.; Chen, Y.; Marceau, C.; Makarov, V.A.; Shkurinov, A.; et al. Analysis of Dual Frequency Interaction in the Filament with the Purpose of Efficiency Control of THz Pulse Generation. *J. Infrared Millim. Terahertz Waves* **2011**, *32*, 1157–1167. [[CrossRef](#)]
16. Dai, J.; Karpowicz, N.; Zhang, X.-C. Coherent Polarization Control of Terahertz Waves Generated from Two-Color Laser-Induced Gas Plasma. *Phys. Rev. Lett.* **2009**, *103*, 023001. [[CrossRef](#)] [[PubMed](#)]
17. Esaulkov, M.N.; Kosareva, O.G.; Makarov, V.; Panov, N.; Shkurinov, A. Simultaneous generation of nonlinear optical harmonics and terahertz radiation in air: Polarization discrimination of various nonlinear contributions. *Front. Optoelectron.* **2015**, *8*, 73–80. [[CrossRef](#)]
18. Zhong, H.; Karpowicz, N.; Zhang, X.-C. Terahertz emission profile from laser-induced air plasma. *Appl. Phys. Lett.* **2006**, *88*, 261103. [[CrossRef](#)]

19. D'Amico, C.; Houard, A.; Franco, M.; Prade, B.; Mysyrowicz, A.; Couairon, A.; Tikhonchuk, V. Conical Forward THz Emission from Femtosecond-Laser-Beam Filamentation in Air. *Phys. Rev. Lett.* **2007**, *98*, 235002. [[CrossRef](#)]
20. Borodin, A.V.; Esaulkov, M.N.; Kuritsyn, I.I.; Kotelnikov, I.A.; Shkurinov, A. On the role of photoionization in generation of terahertz radiation in the plasma of optical breakdown. *J. Opt. Soc. Am. B* **2012**, *29*, 1911–1919. [[CrossRef](#)]
21. You, Y.S.; Oh, T.I.; Kim, K.Y. Off-Axis Phase-Matched Terahertz Emission from Two-Color Laser-Induced Plasma Filaments. *Phys. Rev. Lett.* **2012**, *109*, 183902. [[CrossRef](#)]
22. Oh, T.I.; You, Y.S.; Jhajj, N.; Rosenthal, E.W.; Milchberg, H.M.; Kim, K.Y. Intense terahertz generation in two-color laser filamentation: Energy scaling with terawatt laser systems. *New J. Phys.* **2013**, *15*, 075002. [[CrossRef](#)]
23. Blank, V.; Thomson, M.D.; Roskos, H.G. Spatio-spectral characteristics of ultra-broadband THz emission from two-colour photoexcited gas plasmas and their impact for nonlinear spectroscopy. *New J. Phys.* **2013**, *15*, 075023. [[CrossRef](#)]
24. Gorodetsky, A.; Koulouklidis, A.D.; Massaouti, M.; Tzortzakis, S. Physics of the conical broadband terahertz emission from two-color laser-induced plasma filaments. *Phys. Rev. A* **2014**, *89*, 033838. [[CrossRef](#)]
25. Buccheri, F.; Zhang, X. Terahertz emission from laser-induced microplasma in ambient air. *Optica* **2015**, *2*, 366. [[CrossRef](#)]
26. Andreeva, V.A.; Kosareva, O.G.; Panov, N.A.; Shipilo, D.E.; Solyankin, P.M.; Esaulkov, M.N.; Martínez, P.G.D.A.; Shkurinov, A.P.; Makarov, V.A.; Bergé, L.; et al. Ultrabroad Terahertz Spectrum Generation from an Air-Based Filament Plasma. *Phys. Rev. Lett.* **2016**, *116*, 063902. [[CrossRef](#)]
27. Shkurinov, A.; Sinko, A.S.; Solyankin, P.M.; Borodin, A.V.; Esaulkov, M.N.; Annenkov, V.V.; Kotelnikov, I.A.; Timofeev, I.V.; Zhang, X. Impact of the dipole contribution on the terahertz emission of air-based plasma induced by tightly focused femtosecond laser pulses. *Phys. Rev. E* **2017**, *95*, 043209. [[CrossRef](#)]
28. Stremoukhov, S.Y.; Andreev, A.V. Spatial variations of the intensity of THz radiation emitted by extended media in two-color laser fields. *Laser Phys. Lett.* **2014**, *12*, 15402. [[CrossRef](#)]
29. Ichii, T.; Hazama, Y.; Naka, N.; Tanaka, K. Study of detailed balance between excitons and free carriers in diamond using broadband terahertz time-domain spectroscopy. *Appl. Phys. Lett.* **2020**, *116*, 231102. [[CrossRef](#)]
30. Han, P.; Wang, X.; Zhang, Y. Time-Resolved Terahertz Spectroscopy Studies on 2D Van der Waals Materials. *Adv. Opt. Mater.* **2020**, *8*, 1900533. [[CrossRef](#)]
31. Chai, X.; Ropagnol, X.; Ovchinnikov, A.; Chefonov, O.; Ushakov, A.A.; García-Rosas, C.M.; Isgandarov, E.; Agranat, M.; Ozaki, T.; Savel'ev, A. Observation of crossover from intraband to interband nonlinear terahertz optics. *Opt. Lett.* **2018**, *43*, 5463–5466. [[CrossRef](#)]
32. Point, G.; Brelet, Y.; Houard, A.; Jukna, V.; Milián, C.; Carbonnel, J.; Liu, Y.; Couairon, A.; Mysyrowicz, A. Superfilamentation in Air. *Phys. Rev. Lett.* **2014**, *112*, 223902. [[CrossRef](#)] [[PubMed](#)]
33. Ushakov, A.A.; Chizhov, P.A.; Andreeva, V.A.; Panov, N.A.; Shipilo, D.E.; Matoba, M.; Nemoto, N.; Kanda, N.; Konishi, K.; Bukin, V.V.; et al. Ring and unimodal angular-frequency distribution of THz emission from two-color femtosecond plasma spark. *Opt. Express* **2018**, *26*, 18202. [[CrossRef](#)] [[PubMed](#)]
34. Milián, C.; Jukna, V.; Couairon, A.; Houard, A.; Forestier, B.; Carbonnel, J.; Liu, Y.; Prade, B.; Mysyrowicz, A. Laser beam self-symmetrization in air in the multifilamentation regime. *J. Phys. B At. Mol. Opt. Phys.* **2015**, *48*, 94013. [[CrossRef](#)]
35. Pushkarev, D.; Mitina, E.; Shipilo, D.; Panov, N.; Uryupina, D.; Ushakov, A.; Volkov, R.; Karabutov, A.; Babushkin, I.; Demircan, A.; et al. Transverse structure and energy deposition by a subTW femtosecond laser in air: From single filament to superfilament. *New J. Phys.* **2019**, *21*, 033027. [[CrossRef](#)]
36. Pushkarev, D.; Shipilo, D.; Lar'kin, A.; Mitina, E.; Panov, N.; Uryupina, D.; Ushakov, A.; Volkov, R.; Karpeev, S.; Khonina, S.; et al. Effect of phase front modulation on the merging of multiple regularized femtosecond filaments. *Laser Phys. Lett.* **2018**, *15*, 045402. [[CrossRef](#)]
37. Chu, C.; Shipilo, D.E.; Lu, D.; Zhang, Z.; Chuchupal, S.V.; Panov, N.A.; Kosareva, O.G.; Liu, W. Femtosecond filament emergence between π -shifted beamlets in air. *Opt. Express* **2020**, *28*, 1002–1013. [[CrossRef](#)]
38. Liu, W.; Chin, S.L. Direct measurement of the critical power of femtosecond Ti:sapphire laser pulse in air. *Opt. Express* **2005**, *13*, 5750–5755. [[CrossRef](#)]
39. Panov, N.; Andreeva, V.; Kosareva, O.; Shkurinov, A.; Makarov, V.; Bergé, L.; Chin, S.L. Directionality of terahertz radiation emitted from an array of femtosecond filaments in gases. *Laser Phys. Lett.* **2014**, *11*, 125401. [[CrossRef](#)]
40. Jahangiri, F.; Hashida, M.; Tokita, S.; Nagashima, T.; Hangyo, M.; Sakabe, S. Enhancing the energy of terahertz radiation from plasma produced by intense femtosecond laser pulses. *Appl. Phys. Lett.* **2013**, *102*, 191106. [[CrossRef](#)]